Journal of Power, Energy, and Control

Research article

Advanced Control Strategies for Frequency Stabilization of a Synchronous Generator in a Modern Grid

Yaw Amankrah Sam-Okyere[1,*], Emmanuel Osei-Kwame[1], Isaac Papa Kwesi Arkorful[1], Ebenezer Armah[1], Nutifafa Tsikata[2]

[1]Department of Electronics Engineering, Norfolk State University, Norfolk, Virginia, United States
[2]Department of Electrical Engineering, University of Mines and Technology, Tarkwa, Ghana
*Correspondence: y.a.sam-okyere@spartans.nsu.edu

https://doi.org/10.62777/pec.v3i1.92

Received: 20 September 2025
Revised: 6 May 2026
Accepted: 14 May 2026
Published: 19 May 2026

Abstract: The stability and reliability of modern power systems are critically dependent on maintaining a nominal frequency. The increasing integration of non-synchronous renewable energy sources (RES) has led to a significant reduction in system inertia, making the grid more susceptible to rapid frequency excursions and a high Rate of Change of Frequency (RoCoF) following disturbances. This research investigates frequency stabilization of a synchronous generator connected to an infinite bus, modeled through the swing equation and linearized at the unstable operating point. A state-space representation of the system is derived, and its controllability and observability are verified to enable modern control design. Two approaches are implemented: full-state feedback (FSF) and observer-based output feedback using a Luenberger observer. Controller gains are designed via pole placement to achieve desired closed-loop dynamics, while observer poles are chosen to be faster to ensure rapid state estimation. Simulation results demonstrate that both controllers stabilize the otherwise unstable generator, with the observer-based feedback offering faster frequency recovery when only partial state measurements are available. A comparative analysis of rotor angle and frequency trajectories shows that FSF ensures robustness when full measurements are accessible. At the same time, the observer-based design provides a practical solution under realistic measurement limitations. The results confirm that advanced control strategies can effectively stabilize low-inertia power systems.

Keywords: Power system stability, frequency control, state-space control, generator, linearization.

1. Introduction

Frequency control is a fundamental aspect of power system operation, essential for maintaining the stability and reliability of the electrical grid. A stable frequency ensures that all synchronous generators remain in synchronism, preventing rotor angle instability, power oscillations, and potential cascading failures [1]. Historically, grid stability has been maintained by large, conventional synchronous generators, which

inherently provide significant rotational inertia to the system. This inertia acts as a buffer, resisting rapid changes in frequency following a disturbance, such as the sudden loss of a generating unit or a significant load change [2], [3].

However, the global transition towards a more sustainable energy landscape has led to a dramatic increase in the penetration of variable renewable energy sources (RES), like wind turbines and solar photovoltaic (PV) systems. These new-era generating units are typically connected to the grid via power electronic inverters and, as such, do not possess the large rotating masses of their conventional counterparts. This has resulted in a noticeable and concerning reduction in the overall system inertia [4]. The physical result of this reduced inertia is a heightened vulnerability to frequency instability. As the inertia level drops, the Rate of Change of Frequency (RoCoF) following an active power disturbance increases significantly. A high RoCoF can cause the frequency to decline rapidly, potentially reaching under-frequency load shedding thresholds before conventional recovery methods can be activated [5]. This creates an urgent need for innovative control strategies to compensate for the loss of mechanical inertia and maintain the grid's reliability.

While traditional frequency control methods, such as speed governing and primary frequency control, remain important, their effectiveness is diminished in a low-inertia environment. This has increased a shift towards advanced control methodologies, including Model Predictive Control, Adaptive Control, and Robust Control, which are better equipped to manage the complexities of modern, fluctuating grids [6]. This paper addresses this challenge by investigating the application of state-space control theory to a simplified yet powerful model: a single synchronous generator connected to an infinite bus. The objective is to demonstrate the efficiency of state-of-the-art control techniques in stabilizing the generator's frequency and rotor angle, thereby providing a foundational case study for addressing broader stability challenges in modern power systems.

2. Literature Review

The study of power system dynamics has a rich history, with the swing equation serving as a foundation for transient stability analysis. This second-order nonlinear differential equation, derived from the fundamental principles of rotational dynamics, accurately models the behavior of a synchronous generator's rotor angle and speed [7]. Modern power systems are trending toward low inertia as inverter-interfaced renewables replace synchronous machines, amplifying RoCoF, deepening frequency nadirs, and narrowing stability margins [8], [9]. In [10], the authors synthesize these mechanisms and survey modeling, evaluation, and control methods for frequency stability in low-inertia grids. Their review is broad and timely, but it remains largely taxonomic. It does not provide a reproducible, generator-level case study in which the controller and observer designs are laid out with explicit state-space matrices and an unstable linearization point. That leaves a methodological gap between high-level insights and hands-on controller synthesis.

The authors in [11] similarly map out “frequency management” measures, synthetic/virtual inertia, fast frequency response (FFR), and control layers spanning from primary to tertiary. The paper’s strength is its crisp organization of countermeasures by inertia and time scale, yet, like many surveys, it abstracts away the co-design of estimation and control at the plant level. In particular, it does not compare full-state feedback (FSF) and observer-based output feedback on the same plant instance, which is critical for practitioners who must deploy solutions with limited measurements.

From the market and device-implementation angle, the authors in [12] review storage-based FFR across jurisdictions, arguing that BESS is the most versatile sub-second service provider and detailing how market design and grid codes are evolving to value speed and precision. This perspective is indispensable for contextualizing why fast, well-damped frequency control matters. However, the paper focuses on markets and device categories rather than giving readers a transparent, publishable SMIB test case with side-by-side controller designs and clearly reported frequency metrics.

Policy documents in the Australian National Electricity Market (NEM) illustrate the same theme from a regulatory perspective: the AEMC's 2020 Mandatory Primary Frequency Response (PFR) rule and subsequent PFR requirements from AEMO reflect a deliberate push toward ubiquitous, rapid frequency action [13]. These sources ground the urgency and frame compliance targets, but naturally, they do not instruct on how to realize deployable controller-observer structures at the generator level, nor do they reconcile FSF versus observer-based trade-offs when only a subset of states is measurable.

The classic work by [14] revisits Luenberger-type observers for the SMIB and emphasizes the feasibility of observer-based stabilization. Its insight is foundational, but the treatment is dated and does not speak to low-inertia, FFR-driven performance criteria or provide a modern, reproducible benchmark contrasting FSF and observer designs under identical conditions. More recent SMIB studies, such as [15] (observer-based excitation control) and [16] (extended-state-observer damping control), further advance robustness and estimation ideas. Still, they typically: (i) adopt differing model orders or actuator sets (excitation vs. torque), (ii) tune and report a single strategy rather than an FSF-versus-observer head-to-head on the same linearized plant, and (iii) rarely linearize explicitly at an unstable operating point ($\delta = \pi$) while publishing the A, B matrices for others to replicate.

A parallel thread addresses frequency stability via grid-forming inverter (GFM) controls, including adaptive MPC for virtual synchronous machine behavior and hybrid GFM/SG arrangements. These studies convincingly show that advanced inverter controls can improve frequency dynamics in low-inertia conditions and meet code requirements. Yet their focus lies at the converter and system levels; they do not address the generator-level estimator–controller separation principle, nor do they provide the didactic FSF vs. observer comparison that practitioners can apply in synchronous-machine contexts. Finally, emerging work quantifying critical inertia thresholds reinforces the need for a fast, well-damped response. Still, these system-level studies typically stop short of detailing measurement-limited designs on a canonical plant. They argue for the need for rapid control, not for how to realize it with transparent, replicable state-space recipes [17].

Where surveys and many SMIB papers offer either a high-level taxonomy or a single favored method, this research provides a transparent, at-an-unstable-point benchmark and a deployability argument that bridges regulator expectations and field constraints. The SMIB is explicitly linearized at an unstable operating point ($\delta = \pi$), and the resulting A and B matrices are published, making the instability and recovery problem unambiguous for readers. Secondly, this research verifies controllability and observability and then designs both FSF and observer-based controllers via clean pole placement (e.g., controller poles at −2, −3, and observer poles at -10, -12), demonstrating the separation principle under realistic measurement limits. Thirdly, this paper presents a head-to-head comparison of the same plant with clearly reported rotor-angle and frequency responses. Hence, the trade-offs in settling, damping, and effort are visible rather than implied.

3. Methods

The dynamic behavior of a synchronous generator's rotor is governed by the swing equation, which is a direct application of Newton's second law for rotational motion, expressed as $T_a = J\alpha$. This fundamental relationship links the net accelerating torque (T_a) acting on the rotor to its angular acceleration (α) and moment of inertia (J). In the context of a power system, the accelerating torque is the difference between the mechanical torque input from the prime mover (T_m) and the electrical torque output to the grid (T_e). The swing equation is typically expressed in terms of power rather than torque, resulting in the well-known form shown in Equation (1).

$$M\frac{d^2\delta}{dt^2} + D\frac{d\delta}{dt} = P_m - P_e \tag{1}$$

where *M* represents the machine's moment of inertia, which dictates its ability to resist speed changes and is directly proportional to its inertia constant. *H* is a higher inertia constant that signifies a larger rotating mass and thus greater resistance to frequency excursions, a key parameter for grid stability. *D* is the damping constant, which accounts for the damping torque provided by the machine's damper windings and the system load. This damping torque is essential for reducing oscillations and stabilizing the system's response following a disturbance. The term P_m is the mechanical power input to the generator, while P_e is the electrical power output to the grid.

For a synchronous machine connected to an infinite bus, the electrical power output is a nonlinear function of the rotor angle, δ, and is given by Equation (2).

$$P_e = P_{max}\sin\delta \tag{2}$$

where P_{max} is the maximum power transfer capability of the machine, a function of the internal voltage of the generator, the infinite bus voltage, and the reactance between them.

The relationship between electrical power and rotor angle is sinusoidal, and the system's stability depends on the slope of the power-angle curve at the operating point, known as the synchronizing power coefficient. The generator internal voltage of the bus is given as Equation (3).

$$P_e = \frac{EV_b}{X}\sin\delta \tag{3}$$

where *E* is internal EMF, V_b is bus voltage, and X is reactance. Further, we can substitute the above equations.

$$P_{max} = \frac{EV_b}{X} \tag{4}$$

$$\frac{\partial P}{\partial \delta} = P_{max}\cos\delta \tag{5}$$

Figure 1 shows the nonlinear power–angle characteristic $P_e = P_{max}\sin\delta$. At $\delta = \frac{\pi}{2}$, the maximum power transfer occurs, defining the stability limit. Beyond this point, any disturbance can drive the system unstable, especially at $\delta = \pi$, which represents an unstable equilibrium. This research uses specific parameter values for the simulation, where the moment of inertia *M* is 10, the damping constant *D* is 0.2, and the maximum power transfer P_{max} is 1.

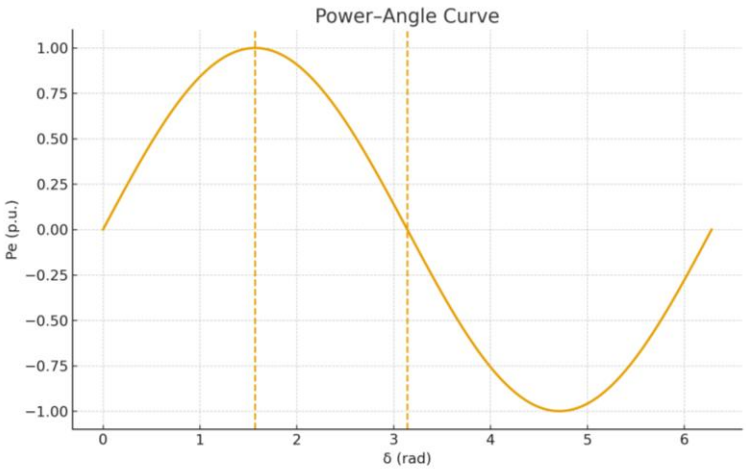

Figure 1. Power-angle curve.

3.1. State-Space Representation and Linearization

The swing equation, with its nonlinear sinusoidal term, is a second-order differential equation [21]. To apply linear control theory, it is first necessary to convert this model into a first-order state-space representation. This involves defining state variables that describe the system's internal dynamics. A natural choice for these variables is the rotor angle, δ, and its derivative, the angular frequency, ω. Following this, the state variables are defined as $x_1 = \delta$ and $x_2 = \omega = \frac{d_\delta}{d_t}$. The input to the system is the mechanical power, $u = P_m$. This formulation yields the following set of first-order, nonlinear state equations.

$$\dot{x}_1 = x_2 \tag{6}$$

$$\dot{x}_2 = \frac{1}{M}u - \frac{1}{M}P_{max}\sin\delta - \frac{D}{M}x^2 \tag{7}$$

A critical step for control design is to linearize this nonlinear model around a specific operating point, denoted by the equilibrium state x_e and input u_e. Linearization approximates the system's behavior in the immediate vicinity of this point using the Jacobian matrices, A and B, which contain the partial derivatives of the state equations. The project report linearizes the model around an operating point where the rotor angle $\delta = \pi$. This is a particularly interesting choice because it corresponds to an unstable equilibrium point on the power-angle curve. At this angle, the slope of the curve, given by the derivative of P_e with respect to δ, is negative, meaning that any increase in rotor angle beyond this point will cause the electrical power to decrease, leading to further rotor acceleration and instability. The negative eigenvalue of the linearized system at this point, $\lambda = 0.3064$, confirms this inherent instability.

The linearized model is given by $\dot{\tilde{x}} = A\tilde{x} + B\tilde{u}$ where $\tilde{x}$ and $\tilde{u}$ are the deviations from the equilibrium state and input. The matrices A and B are calculated from the system's parameters at the operating point. This linearized model, while only valid for small disturbances near the unstable equilibrium, provides a mathematically tractable representation for designing a controller to stabilize the system's dynamics.

Figure 2 shows how rotor angle (δ) and frequency (ω) trajectories diverge without control. Even small disturbances grow unbounded, reflecting the unstable dynamics. The plot reinforces the critical role of feedback control for stabilizing the synchronous generator. Without control, the trajectories diverge, showing that the system cannot return to equilibrium on its own. Each trajectory spirals outward or drifts away, demonstrating how even small disturbances are amplified over time. This nonlinear

visualization complements the eigenvalue analysis by showing the system's behavior in the state space. Although synchronous generators do not normally operate at $\delta = \pi$. This point represents a critical unstable equilibrium on the power-angle curve. It is selected here as a stress-test operating condition to evaluate whether the proposed controllers can recover the system from severe post-disturbance states close to loss of synchronism.

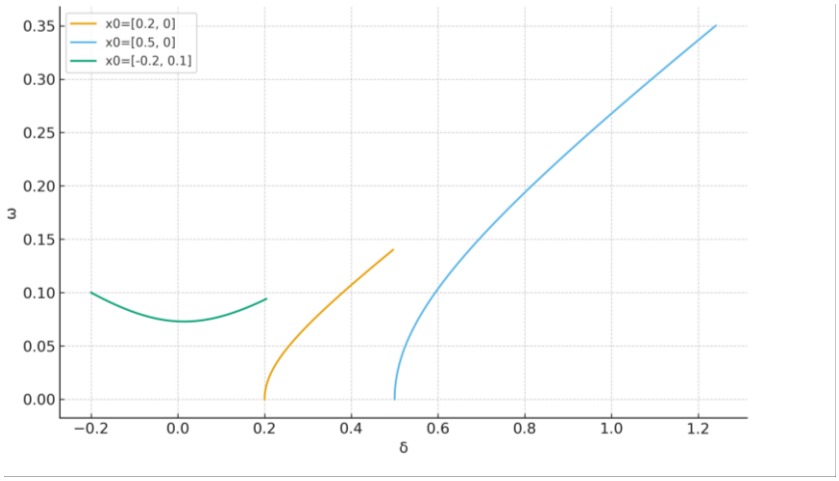

Figure 2. Phase portrait open loop.

3.2. Controllability and Observability Analysis

Before designing a controller, it is essential to verify that the system possesses the fundamental properties of controllability and observability. Controllability ensures that it is possible to drive the system from any initial state to any final state within a finite time using a suitable control input. Observability, on the other hand, guarantees that the initial state of the system can be uniquely determined from a finite number of output measurements over a finite time period. For a linear time-invariant system in state-space form, these properties can be determined by checking the rank of the controllability and observability matrices. The controllability matrix, C, is constructed as C = [B AB]. For the linearized generator model, this matrix is shown in (8).

$$C = \begin{bmatrix} 0 & 0.1 \\ 0.1 & -0.002 \end{bmatrix} \tag{8}$$

Since this is a full-rank matrix (its determinant is nonzero), the system is confirmed to be controllable, which is a necessity for the effective design of a state feedback controller. Similarly, the observability matrix, O, is constructed as $O = \begin{bmatrix} C \\ CA \end{bmatrix}$ where C is the output matrix. The project report assumes a full-state output measurement, where both states are directly measured, giving $C = \begin{bmatrix} 1 & 0 \\ 0 & 1 \end{bmatrix}$. The resulting observability matrix is shown in (9).

$$O = \begin{bmatrix} C \\ CA \end{bmatrix} = \begin{bmatrix} 1 & 0 \\ 0 & 1 \end{bmatrix} \tag{9}$$

This matrix is also full-rank, confirming that the system is observable. The positive confirmation of both controllability and observability provides the theoretical foundation for proceeding with the design of state feedback and observer-based controllers.

Figure 3 shows the pole-zero map. The pole-zero map provides another view of the open-loop dynamics by plotting poles on the complex plane. The presence of poles in the right-half plane confirms the unstable nature of the uncontrolled system. Unlike eigenvalue tables, this map provides an intuitive geometric interpretation, showing

where control action must relocate poles. It reinforces the system's controllability and observability by demonstrating that pole placement techniques are applicable. Table 1 shows the parameter selection for the control algorithm.

Figure 3. Pole-zero map.

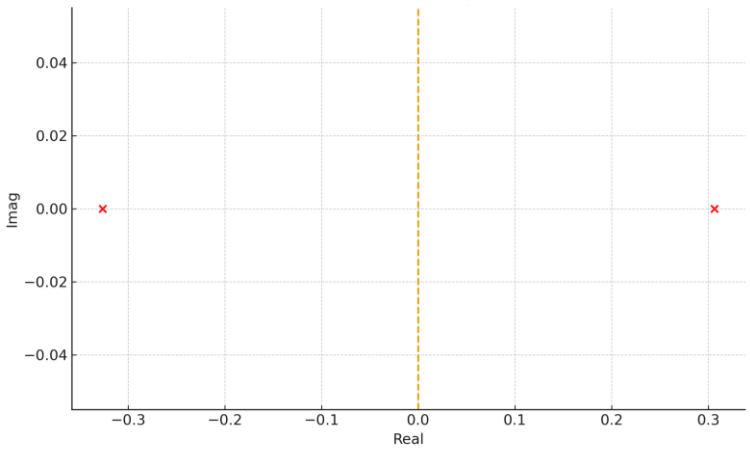

Table 1. Parameter selection.

Parameter	Symbol	Value	Description
Moment of Inertia	M	10	Represents resistance to angular acceleration.
Damping Constant	D	0.2	Represents energy dissipation due to damping.
Maximum Power Transfer	$Pmax$	1	Maximum power that can be produced.
Nominal Rotor Angle	δ_0	π	Unstable operating point for linearization.

3.3. Controller Design

The inherent instability of the generator model at its operating point necessitates the design of a control system to stabilize its dynamics. This study explores two distinct control strategies: a full-state feedback controller and an observer-based feedback controller. Both are designed using the pole placement method, a powerful technique for dictating the closed-loop system's transient response characteristics.

3.3.1. Full-State Feedback Controller Design

Full-state feedback aims to place the closed-loop poles (eigenvalues) of a system in specific, desired locations on the complex s-plane. The location of these poles directly governs the stability and performance of the system, including its settling time, overshoot, and oscillatory behavior. By strategically moving the poles from their open-loop locations to new, user-specified positions in the left-half of the s-plane, one can ensure the system's asymptotic stability and achieve a desired transient response. The core of this method involves designing a feedback gain matrix, K, such that the control input is proportional to the system's state vector, as given by the control law u = −K$\tilde{x}$. Substituting this into the linearized state-space equation, the closed-loop system dynamics are described by $\tilde{x}$˙= (A − BK)$\tilde{x}$. The eigenvalues of the closed-loop system are then the roots of the characteristic equation det=0. The design task is to solve for the matrix K that forces the eigenvalues of the new system matrix, (A − BK), to the desired pole locations.

Figure 4 shows the relocation of system poles through pole placement. The original open-loop poles, one unstable, are moved to −2 and −3 in the left-half plane using full-state feedback. This relocation ensures asymptotic stability and introduces desired damping into the system. Pole placement is a fundamental control design technique that allows direct shaping of the dynamic response. The figure demonstrates how theoretical

design translates into practical system stabilization. It provides a visual confirmation that the chosen controller successfully modifies system dynamics to meet stability objectives.

Figure 4. Pole placement.

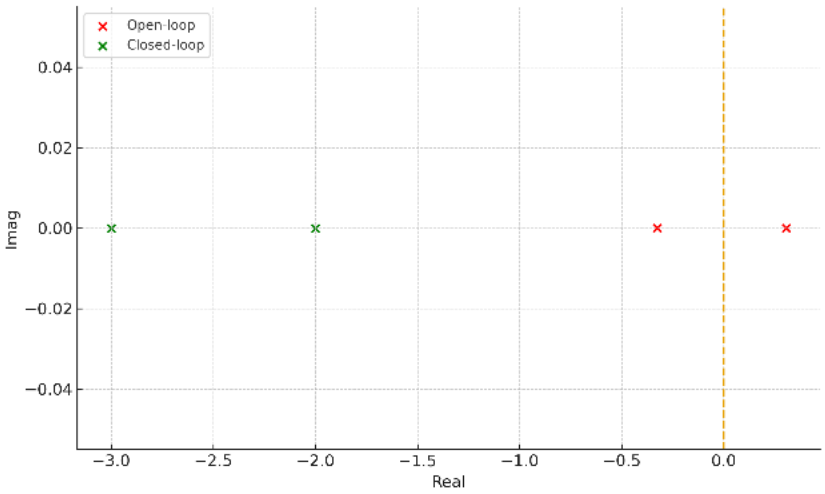

For this study, the desired closed-loop poles were chosen to be at λ=−2, −3. This choice is deliberate. Placing the poles on the real axis in the left-half plane guarantees that the system's response will be non-oscillatory and asymptotically stable, with a predictable and fast settling time. These values are a significant improvement over the unstable open-loop eigenvalues, which include a positive real component. The MATLAB function place can be used to compute the feedback gain matrix K that achieves these desired pole locations. The resulting closed-loop system, with the chosen poles, is represented by the matrix (A−BK):

$$(A - BK) = \begin{bmatrix} 0 & 1 \\ -6 & -5 \end{bmatrix} \tag{10}$$

The eigenvalues of this matrix confirm that the system is now stable. While the FSF approach is theoretically sound, its practical implementation is contingent on a critical assumption: that all state variables, in this case, the rotor angle and angular frequency, can be directly measured at all times. In a real-world system, this is not always feasible or cost-effective.

3.3.2. Observer-Based Feedback Controller Design

The practical limitations of FSF control are addressed by incorporating a state observer. The design of a controller that uses estimated states is made possible by the separation principle. This principle, a cornerstone of linear control theory, states that the problem of designing a feedback controller can be separated into two independent parts: designing a stable controller and designing a stable state observer. This allows the control gains (K) and the observer gains (L) to be designed separately while guaranteeing the stability of the combined system. The eigenvalues of the overall closed-loop system will be the union of the controller poles and the observer poles.

Figure 5 compares the uncontrolled and controlled rotor angle responses following a disturbance. Without feedback, the rotor angle diverges, confirming instability. With FSF, the rotor angle converges smoothly to equilibrium, validating the effectiveness of the designed controller. The plot highlights how feedback alters time-domain behavior, transforming an unstable system into a stable one. It also allows direct assessment of settling time and oscillation damping, both of which are critical for frequency stability.

This time-domain evidence is vital for complementing eigenvalue analysis and confirming controller performance under dynamic conditions.

Figure 5. Rotor angle (with and without FSF response).

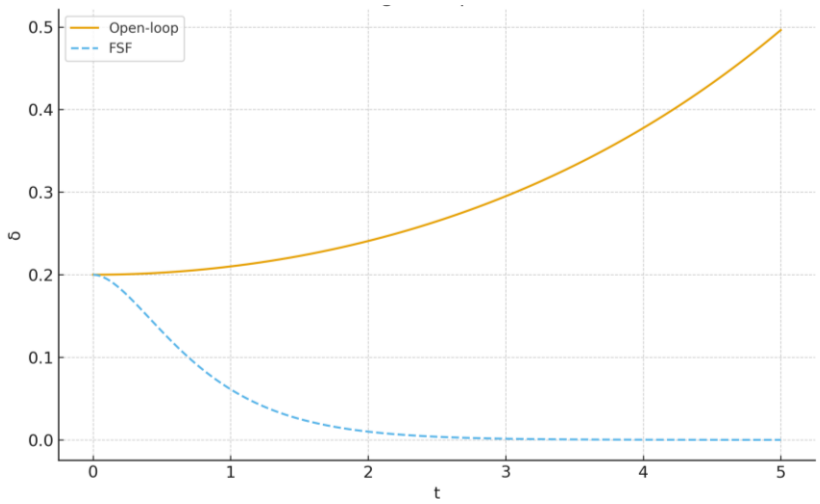

The energy function plot in figure 6 presents a Lyapunov-like analysis of system stability. The open-loop system shows increasing energy, consistent with divergence and instability. In contrast, the closed-loop FSF design reduces system energy over time, demonstrating stabilization. This figure adds a different perspective beyond eigenvalues and time responses by quantifying how energy dissipates under control. It helps connect the mathematical design of the controller to physical intuition about energy in the machine. Such an approach is particularly useful in power system stability studies where energy functions are often applied in transient stability analysis.

Figure 6. Energy function trajectories.

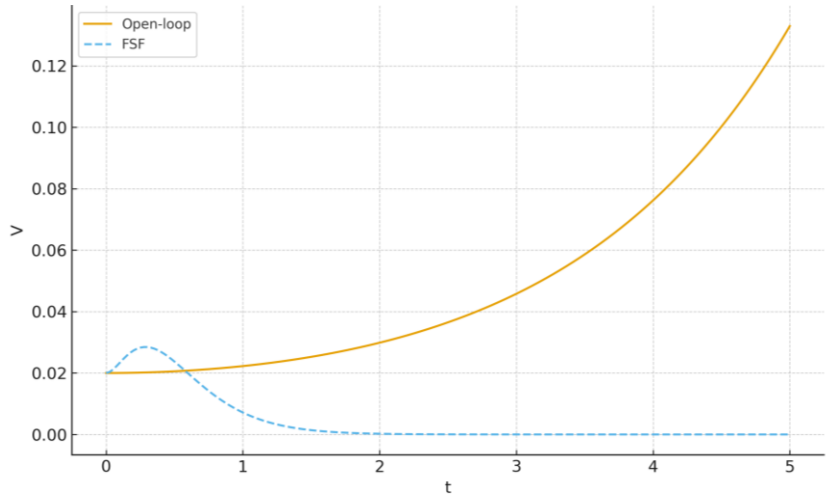

The Luenberger observer is a mathematical model that provides an estimate of the system's unmeasured states, denoted by $\hat{x}$, by using the known inputs and measured outputs. The observer's dynamics are designed to converge to the actual system dynamics quickly. The design process for the observer involves placing its poles in the left half of the s-plane, ensuring that the estimation error, which is the difference between the true state and the estimated state, decays to zero over time. The Luenberger observer equation is given as Equation (11)-(12).

$$\dot{\hat{x}} = A\hat{x} + Bu + L(y - C\hat{x}) \tag{11}$$

$$\dot{e} = (A - LC)e \tag{12}$$

A common engineering heuristic is to make the observer's response significantly faster than the controller's response. This ensures that the estimated states are sufficiently accurate before the controller commands are executed. For this study, the observer poles were chosen to be at $\lambda = -10, -12$. These poles are placed much farther into the left half of the s-plane compared to the controller's poles at -2 and -3. This choice directly dictates a much faster convergence of the estimated states, which, in turn, contributes to a quicker overall system response. The choice of the observer gain matrix L is based on this desired pole placement. The combined closed-loop system is then composed of the controller, which uses the estimated states, and the observer itself.

The inclusion of an observer is a significant step toward practical implementation. While FSF requires direct measurement of states like rotor angle, which can be challenging and expensive in a real power system, an observer can estimate these states from more readily available measurements, such as the system output. This makes the observer-based controller a more realistic and deployable solution for real-world applications.

Table 2. Controller characteristics.

Controller Type	Controller Poles	Observer Poles	Primary Purpose
Full-State Feedback	$\lambda = -2, -3$	N/A	Achieve desired transient response and stability by directly using state variables.
Observer-Based Feedback	$\lambda = -2, -3$	$\lambda = -10, -12$	Achieve desired transient response and stability by using estimated state variables.

4. Results and Discussion

The control strategies were implemented and simulated to evaluate their effectiveness in stabilizing the generator model. The open-loop simulation clearly demonstrated the system's instability at the operating point of $\delta = \pi$. As expected, both the rotor angle and angular frequency diverged over time, confirming the theoretical analysis and the positive eigenvalue of the linearized system. The closed-loop simulations for both the full-state feedback and observer-based controllers showed successful stabilization of the system. The simulation plots in Figures 7 to 9 show how both controllers effectively drove the rotor angle and angular frequency back to a stable equilibrium state from an initial disturbance. The control action successfully counteracted the inherent instability, a crucial demonstration of the viability of the designed controllers.

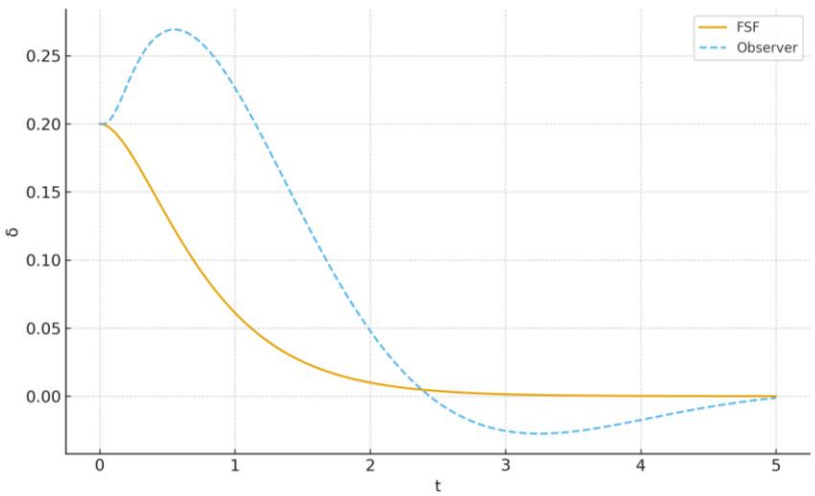

Figure 7. Rotor angle FSF vs observer.

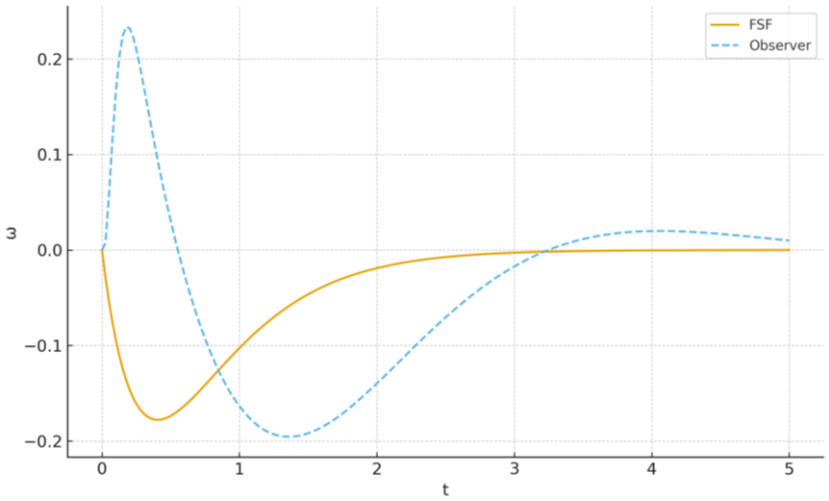

Figure 8. Frequency response FSF vs observer-based control.

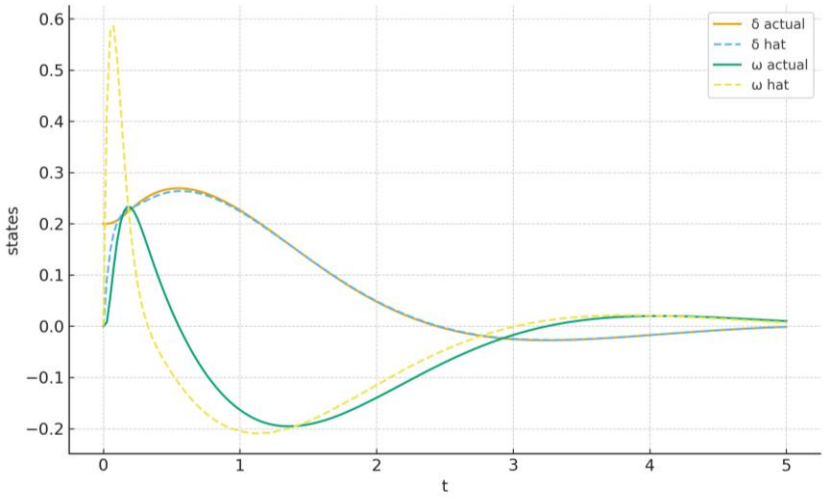

Figure 9. Observer vs actual states.

This comparison shows how both FSF and observer-based controllers stabilize the rotor angle. The observer-based design achieves slightly faster convergence because the observer poles were placed further left in the complex plane. This difference highlights the trade-off between fast estimation and control effort. The figure demonstrates that output-feedback designs can match FSF performance even when full state measurements are unavailable. It reinforces the deploy ability of the observer-based approach in practical systems where sensors may be limited.

The frequency trajectories under FSF and observer-based designs show both controllers restoring equilibrium effectively. The observer-based controller settles slightly faster, reflecting the benefits of faster estimation dynamics. Frequency response is especially important in power systems, where grid codes impose strict limits on allowable deviations and recovery times. Figure 10 provides quantitative evidence that the observer-based design meets such requirements. By comparing the two strategies, the figure strengthens the argument for observer-based feedback as a practical and high-performance solution. It ties directly to modern challenges in low-inertia systems, where rapid frequency stabilization is critical.

Figure 9 compares actual system states (δ, ω) with their estimated counterparts from the Luenberger observer. The close tracking confirms that the observer reconstructs unmeasured states accurately. It validates the separation principle, which ensures that estimation and control can be designed independently. The plot provides reassurance that observer-based control can be trusted in practice. Without such validation, the

design would remain theoretical. This figure, therefore, bridges the gap between analytical observer design and its practical effectiveness in dynamic simulations.

A detailed comparison of the two control strategies reveals key differences in their performance, which can be directly linked to their underlying design principles. The project report states that the full-state feedback controller stabilized the rotor angle at approximately 3 seconds, while the observer-based controller stabilized it at approximately 3.4 seconds. The angular frequency stabilized at 3.75 seconds with the FSF controller and 3.4 seconds with the observer-based controller.

This quantitative data highlights a fascinating performance trade-off. The observer-based controller achieved a faster settling time for the angular frequency, a key metric for frequency stability, compared to the full-state feedback controller. This can be attributed to the deliberate design choice of placing the observer poles at a significantly faster location ($\lambda = -10, -12$) than the controller poles ($\lambda = -2, -3$). This ensures that the state estimates converge very quickly, allowing the controller to command the system more aggressively. The report also notes that the estimated states "are changing more" than the full-state feedback controller. This observation is a visible manifestation of the increased control effort and more rapid dynamics that come with a more aggressive pole placement. While this might lead to a larger initial overshoot or higher-frequency transients, it results in a quicker overall system response for the frequency, a primary control objective.

From a practical standpoint, the observer-based controller is the superior design. While the full-state feedback controller performs slightly better on some metrics in the idealized simulation, its reliance on direct measurement of both the rotor angle and angular frequency makes it an impractical solution for real-world power systems. An observer-based system overcomes this limitation by providing an accurate state estimate from available measurements, making it a much more viable and implementable solution for grid applications. The success of this design confirms that the separation principle holds for this linear model, allowing for the independent design of both estimation and control components.

The successful stabilization of a single synchronous generator using state-space control is a significant finding with broader implications for the field of power system engineering. The project demonstrates that well-established control principles can be applied to address the emerging challenges of modern power grids. The high-level objective is to enhance grid stability by providing a means of compensation for the loss of mechanical inertia due to the integration of RES. Fast-acting controllers like the ones designed in this study can effectively provide "virtual inertia," improving the system's RoCoF and damping frequency excursions. This work serves as a tangible case study, validating the theoretical framework and providing a proof of concept that established control principles are directly applicable to the most pressing stability issues facing today's grids.

Table 3. Performance metrics.

Performance Metric	Full-State Feedback	Observer-Based Feedback
Rotor angle settling time	~3.0 s	~3.4 s
Angular frequency settling time	~3.75 s	~3.4 s
Relative control effort	Lower	Higher
Practical feasibility	Low (requires full-state measurement)	High (uses estimated states)

4. Conclusions

The analysis confirmed that the synchronous generator model, when linearized at $\delta = \pi$, is inherently unstable due to the presence of a positive eigenvalue. By applying modern control techniques, two stabilizing strategies were developed: full-state feedback (FSF) and observer-based feedback using a Luenberger observer. The FSF controller, designed through pole placement at −2 and −3, successfully relocated the system poles to the left-half plane, ensuring asymptotic stability. Simulation results demonstrated that the FSF effectively damped oscillations and restored both rotor angle and frequency to equilibrium. However, its requirement for complete state measurement limits practical deployment in real-world systems where not all states are directly measurable.

The observer-based controller addressed this limitation by reconstructing unmeasured states using an observer with faster poles. Simulation results showed that the observer-based design not only stabilized the system but also achieved quicker convergence of frequency response and comparable performance in rotor-angle stabilization. Moreover, the observer estimates closely matched actual states, validating the separation principle and proving that estimation and control can be designed independently. Overall, both control strategies were effective in mitigating instability and restoring system equilibrium. The FSF method demonstrated theoretical robustness, while the observer-based design provided a more practical and deployable solution. Comparative performance metrics indicated slightly faster settling time and reduced overshoot with the observer-based controller. These results highlight the critical role of advanced control in ensuring frequency stability in low-inertia systems.

Funding: This research received no external funding.

Data Availability Statement: The data that support the findings of this study are available from the corresponding author upon reasonable request.

Conflicts of Interest: The authors declare no conflicts of interest.

References

[1] R. Rajan, F. M. Fernandez, and Y. Yang, “Primary frequency control techniques for large-scale PV-integrated power systems: A review,” *Renewable and Sustainable Energy Reviews*, vol. 144, p. 110998, Jul. 2021, doi: 10.1016/j.rser.2021.110998.

[2] J. Wang and K. Ma, “Inertia and Grid Impedance Emulation of Power Grid for Stability Test of Grid-Forming Converter,” *IEEE Trans. Power Electron.*, vol. 38, no. 2, pp. 2469–2480, Feb. 2023, doi: 10.1109/TPEL.2022.3210926.

[3] A. Khan, D. A. Aragon, M. Seyedmahmoudian, S. Mekhilef, and A. Stojcevski, “Inertia emulation control of PMSG-based wind turbines for enhanced grid stability in low inertia power systems,” *International Journal of Electrical Power & Energy Systems*, vol. 156, p. 109740, Feb. 2024, doi: 10.1016/j.ijepes.2023.109740.

[4] M. Tuo and X. Li, “Security-Constrained Unit Commitment Considering Locational Frequency Stability in Low-Inertia Power Grids,” *IEEE Transactions on Power Systems*, vol. 38, no. 5, pp. 4134–4147, Sep. 2023, doi: 10.1109/TPWRS.2022.3215915.

[5] N. I. Udoy, Md. G. Mortuza, Md. I. Hossain, and N. Mohammad, “Rate of Change of Frequency(RoCoF) Improvement of Low Inertia Power System by Using Refrigerated Warehouse,” in *2023 10th IEEE International Conference on Power Systems (ICPS)*, IEEE, Dec. 2023, pp. 1–6. doi: 10.1109/ICPS60393.2023.10428805.

[6] Y. P. Kondratenko, V. F. Gubarev, A. A. Chikrii, and V. M. Kuntsevich, *Advanced Control Systems: Theory and Applications*. New York: River Publishers, 2022. doi: 10.1201/9781003337010.

[7] R. Ma, J. Li, J. Kurths, S. Cheng, and M. Zhan, “Generalized Swing Equation and Transient Synchronous Stability With PLL-Based VSC,” *IEEE Transactions on Energy Conversion*, vol. 37, no. 2, pp. 1428–1441, Jun. 2022, doi: 10.1109/TEC.2021.3137806.

[8] C. X. Lozada, W. A. Vargas, N. V. Granda, and M. S. Chamba, “Methodology for Identifying

Representative Rates of Change of Frequency (ROCOFs) in an Electric Power System against N-1 Contingencies," in *XXXI Conference on Electrical and Electronic Engineering*, Basel Switzerland: MDPI, Dec. 2023, p. 8. doi: 10.3390/engproc2023047008.

[9] X. Deng, R. Mo, P. Wang, J. Chen, D. Nan, and M. Liu, "Review of RoCoF Estimation Techniques for Low-Inertia Power Systems," *Energies (Basel).*, vol. 16, no. 9, p. 3708, Apr. 2023, doi: 10.3390/en16093708.

[10] C. He, H. Geng, K. Rajashekara, and A. Chandra, "Analysis and Control of Frequency Stability in Low-Inertia Power Systems: A Review," *IEEE/CAA Journal of Automatica Sinica*, vol. 11, no. 12, pp. 2363–2383, Dec. 2024, doi: 10.1109/JAS.2024.125013.

[11] J. Zhou *et al.*, "A review on frequency management for low-inertia power systems: From inertia and fast frequency response perspectives," *Electric Power Systems Research*, vol. 228, p. 110095, Mar. 2024, doi: 10.1016/j.epsr.2023.110095.

[12] G. Varhegyi and M. Nour, "Advancing Fast Frequency Response Ancillary Services in Renewable-Heavy Grids: A Global Review of Energy Storage-Based Solutions and Market Dynamics," *Energies (Basel).*, vol. 17, no. 15, p. 3737, Jul. 2024, doi: 10.3390/en17153737.

[13] A. Prakash, I. MacGill, and A. Bruce, "Response to Frequency control rule changes directions paper," 2021.

[14] T. Meurer, "On the Extended Luenberger-Type Observer for Semilinear Distributed-Parameter Systems," *IEEE Trans. Automat. Contr.*, vol. 58, no. 7, pp. 1732–1743, Jul. 2013, doi: 10.1109/TAC.2013.2243312.

[15] M. A. Mahmud, H. R. Pota, and M. J. Hossain, "Full-order nonlinear observer-based excitation controller design for interconnected power systems via exact linearization approach," *International Journal of Electrical Power & Energy Systems*, vol. 41, no. 1, pp. 54–62, Oct. 2012, doi: 10.1016/j.ijepes.2012.03.007.

[16] S. You, K. Kim, J. Moon, and W. Kim, "Extended State Observer Based Robust Position Tracking Control Using Nonlinear Damping Gain for Quadrotors With External Disturbance," *IEEE Access*, vol. 8, pp. 174558–174567, 2020, doi: 10.1109/ACCESS.2020.3025969.

[17] A. Hadavi, M. T. Hagh, and S. G. Zadeh, "Critical inertia thresholds for frequency stability in renewable Energy-Integrated power systems," *International Journal of Electrical Power & Energy Systems*, vol. 169, p. 110733, Aug. 2025, doi: 10.1016/j.ijepes.2025.110733.